

Accepted Manuscript

Title: Marine Salinity Sensing Using Long-period Fiber Gratings Enabled by Stimuli-responsive Polyelectrolyte Multilayers

Authors: Fan Yang, Svetlana Sukhishvili, Henry Du, Fei Tian



PII: S0925-4005(17)31140-1
DOI: <http://dx.doi.org/doi:10.1016/j.snb.2017.06.121>
Reference: SNB 22592

To appear in: *Sensors and Actuators B*

Received date: 19-1-2017
Revised date: 15-6-2017
Accepted date: 17-6-2017

Please cite this article as: Fan Yang, Svetlana Sukhishvili, Henry Du, Fei Tian, Marine Salinity Sensing Using Long-period Fiber Gratings Enabled by Stimuli-responsive Polyelectrolyte Multilayers, *Sensors and Actuators B: Chemical* <http://dx.doi.org/10.1016/j.snb.2017.06.121>

This is a PDF file of an unedited manuscript that has been accepted for publication. As a service to our customers we are providing this early version of the manuscript. The manuscript will undergo copyediting, typesetting, and review of the resulting proof before it is published in its final form. Please note that during the production process errors may be discovered which could affect the content, and all legal disclaimers that apply to the journal pertain.

Marine Salinity Sensing Using Long-Period Fiber Gratings Enabled by Stimuli-Responsive Polyelectrolyte Multilayers

Fan Yang,¹ Svetlana Sukhishvili,² Henry Du,¹ Fei Tian,^{1,*}

¹Department of Chemical Engineering and Materials Science, Stevens Institute of Technology, Hoboken, NJ 07030

²Department of Materials Science and Engineering, Texas A&M University, College Station, Texas 77843

*Corresponding author: ftian1@stevens.edu

Abstract

A highly sensitive fiber-optic salinity sensor synergistically combining long-period gratings (LPG) and stimuli-responsive polyelectrolyte multilayers is demonstrated. The LPG coupled with LP_{0,10} cladding mode was coated with ionic-strength-responsive chitosan (CHI)/poly (acrylic acid) (PAA) polyelectrolyte multilayers *via* the layer-by-layer (LbL) assembly technique. This LbL-coated LPG was exposed to NaCl solutions with varying concentrations for salinity measurement. The LPG resonance wavelength underwent a change from red shift to blue shift at the salt concentration of 0.5 M over the 0.1-0.8 M range at pH 7.5. A significant blue shift with a sensing response of 36 nm/M was observed from 0.5 to 0.8 M, relevant to that of seawater. This sensitivity is one order of magnitude higher than that obtained using as fabricated LPG without the stimuli-responsive LbL multilayers as well as documented studies. The mechanism associated with the salinity response of the LbL multilayers is discussed.

Keywords: Fiber-optic sensors; ; ; , Salinity, Long period gratings, Polyelectrolytes, Layer-by-layer assembly

1. Introduction

Real-time monitoring of salt concentration in aqueous solution is in increasing demand for a variety of sectors ranging from life sciences, agriculture to climate and marine studies. For example, maintaining specific salt concentrations is important for vital functions of many animals and plants, and is critical for shellfish productivity and algal blooms [1]. Salinity measurements are also crucial in climate change research, as they provide essential information on factors influencing global weather such as ocean

circulation and water mass movements [2]. It is known that the passage of sound in seawater is dependent on its density and salinity. Activities involving sonar devices rely on an accurate measurement of salinity in applications including seabed mapping, submarine detection and bathymetry [3]. Other traditional ways to measure salinity are chemical or electrical methods which usually require high maintenance, as seen in the case of titration with silver nitrate or electrical conductivity [4]. It is thus of great scientific and engineering significance to develop more robust salinity sensors with the potential of remote and real-time measurement, ease of integration with fiber-optic network, automation, immunity to environmental degradation and electromagnetic field, high sensitivity and reduced size and cost.

Fiber-optic salinity sensors are ideal candidates to meet the aforementioned multiple requirements. The technique has the capability of real-time remote monitoring and can be easily adapted for multiplexing for multi-parameter sensing [5, 6, 7]. Salinity fiber sensors typically measure the refractive index (RI) of the saline water so a highly RI-sensitive optical fiber sensor is of great appeal for salinity sensing [8], with long period gratings as a good example of fiber optic grating based sensors [9, 10]. A long period grating (LPG) couples the light from the fundamental core mode to the co-propagating cladding mode at well-defined resonance wavelengths (RW) [11]. The phase matching condition is determined by $\lambda_{\text{resonance}} = (n_{\text{eff, core}}^{\text{eff}} - n_{\text{eff, cladding}}^{\text{eff}})\Lambda$, where, $\lambda_{\text{resonance}}$ is the coupling RW of the cladding mode, $n_{\text{eff, core}}^{\text{eff}}$ and $n_{\text{eff, cladding}}^{\text{eff}}$ are respective effective indices of the core and the cladding modes, and Λ is grating period [11, 12]. The dependence of $\lambda_{\text{resonance}}$ on $n_{\text{eff, core}}^{\text{eff}}$ and $n_{\text{eff, cladding}}^{\text{eff}}$ makes LPG a highly sensitive index transduction platform [13]. An attempt to improve the RI sensitivity of LPG with an in-fiber Mach-Zehnder interferometer based on two cascaded LPGs for salinity measurement was reported [14]. Despite the vast advantages fiber-optic salinity sensor may offer, to date, this type of salinity sensors either has very low salinity sensitivity with only 2 nm shift/ M [15] as an example or involved metal coating [16] with vulnerability to corrosion due to a high concentration of salt ions. Recent effort of incorporating responsive or “intelligent” functional thin film

with LPG [17] for pH sensing has inspired the development of a highly sensitive salinity sensor assisted by an ionic-strength-responsive polyelectrolyte multilayer via layer-by-layer (LbL) assembly. LbL, generally referred to as the sequential alternating deposition procedure involving oppositely charged polyelectrolytes [17], is a promising way to conformably construct functional thin films on substrates with a wide range of chemical natures and shapes including colloidal particles, fluidic interfaces and liposomes, to name a few [18].

In this study, we explore the integration of ionic-strength-responsive chitosan (CHI)/poly (acrylic acid) (PAA) multilayers with LPG for salinity sensing. The LbL assembly, driven by electrostatic interactions between the polyelectrolyte counter ions, was monitored in real time till desired number of CHI/PAA layers was deposited on LPG. The LPG response to the deposition of [CHI/PAA]₂₀ was recorded as a RW shift. The LPG coated with films deposited at a low concentration of salt was subsequently exposed to NaCl solutions from 0.1 to 0.8M, especially high concentration encompassing that of marine seawater and salt lakes from 0.5 M to 0.8 M at pH 7.5 [19, 20]. A high salinity sensitivity was achieved with the aid of the [CHI/PAA]_n multilayers in response to ionic strength of salinity solution and the subsequent change in the external RI around the LPG. The paper provides significant insights into the mechanism of sensor response that is centered around the ionic-strength-induced swelling/de-swelling of [CHI/PAA]_n films.

2. Material and methods

2.1. Chemical reagents and materials

Sodium chloride (NaCl), sodium hydroxide standard solution (0.1 M, NaOH), poly (acrylic acid) (PAA, Mw ~450 kDa), chitosan (CHI, high purity, Mw ~60-120 kDa), 3 M sodium acetate buffer (NaOAc), sodium dihydrogen phosphate (NaH₂PO₄), disodium phosphate (Na₂HPO₄) and hydrogen

tetrachloroaurate (III) (30 wt % solution in dilute hydrochloric acid, 99.999%) were obtained from Sigma-Aldrich. Hydrochloric acid (1 N standard solution, HCl) was purchased from Acros Organics. Hydrogen peroxide (30% in water, H₂O₂) and sodium citrate were obtained from Fisher Scientific Inc. All chemicals were used without any further purification steps. All solutions were prepared using ultrapure water (Milli-Q ultrapure water (<18.2 MΩ•cm)). Both CHI and PAA solutions were prepared with a concentration of 2 mg/mL in 100 mM sodium acetate (NaOAc) buffer and adjusted to a pH 5.0 during the deposition process. The 0.01 M phosphate buffer solutions of pH 7.5 were pH adjusted with NaOH and HCl. The salinity solutions were prepared by adding sodium chloride powder to the phosphate buffer solutions.

2.2. LPG fabrication

The LPG was fabricated using point-by-point irradiation of a focused CO₂ laser beam. The CO₂ laser with a closed loop kits has excellent power stability (<1%) to guarantee reproducible LPG structure. We inscribed LPG of high order cladding mode LP_{0,10} with the aid of 120° Au-coated Si reflection mirror pair via a motorized translation stage with 0.2 μm minimum incremental motion. The entire LPG fabrication is controlled by computer interface to ensure synchronized operations on laser irradiation and translation stage. The employed optical fiber was SMF-28 (from Corning Optical Communications Inc.). The LPG coupled with LP_{0,10} cladding mode was fabricated with parameters of 247 μm in grating period and 5 cm in length. A broadband light source was connected to one end of the LPG and an optical spectrum analyzer (OSA) to the other for the measurement of the transmission spectra of the LPG in real time during the fabrication process.

2.3. Coating deposition

LPG fiber was mounted and fastened between two holders on an optical stage. It was dipped into a container with a V-shaped groove holding the polyelectrolyte solutions during the LbL assembly. Briefly,

LPG was cleaned with 7.5% H_2O_2 solution for 20 min before LbL deposition. Polyelectrolyte thin films were deposited at room temperature by alternately dipping the LPG fiber in the V-shaped groove containing positively charged CHI solution for 5 min followed by two consecutive rinse steps in 100 mM sodium acetate buffer for 2 min, and then into a negatively charged PAA solution for 5 min followed by the same rinse cycle. The solutions were injected and aspirated by syringes. The entire deposition process was repeated 20 times, establishing a polyelectrolyte multilayer of $[\text{CHI}/\text{PAA}]_{20}$ on the surface of LPG. The whole process was monitored by the LPG after the deposition of each layer. All polyelectrolyte solutions and rinsing buffer were pH-adjusted to 5.0 during the deposition process. When the deposition process was completed, the coated LPG was immersed in phosphate buffer solution at pH 7.5 until the coating was stabilized and dried at room temperature.

In order to characterize the deposition process, we deposited the polyelectrolyte multilayers on Au nanoparticles (NPs) and obtained the zeta-potential measurement after the deposition of each and every individual layer. For deposition of CHI/PAA films on colloidal particles, 0.2 mL of 1 mg/mL CHI solution was added to 0.8 mL of 0.39 mg/mL colloidal solution of Au NPs 100 nm in diameter [21]. After incubation for 12 h, Au NPs were centrifuged and washed with NaOAc buffer at pH 5 for three times. The same procedure was repeated for PAA. The process was repeated until desired layer number of $[\text{CHI}/\text{PAA}]_n$ was assembled. The coated colloidal dispersion was finally purified by centrifugation and re-dispersed in NaOAc buffer at pH 5.

3. Results and discussion

3.1. Layer by layer assembly

The transmission spectra of the LPG for the CHI/PAA LbL deposition are shown in Fig. 1. Each deposition step increases the thickness of the thin film, resulting in a change in the effective external RI and a corresponding red shift in the RW of the LPG. The large red shift obtained during LbL deposition is a

strong evidence of the feasibility and promise of our LPG platform for the real-time monitoring of LbL events. The average thickness of [CHI/PAA]₂₀ multilayers is about 3.3 micrometers, as can be seen from the cross-sectional scanning electron microscope (SEM) images in Fig. 2.

Fig. 1. LPG transmission spectra for the monitoring of the LbL assembly of CHI/PAA multilayers on SMF-28 with LPG at pH 5.

Fig. 2. The cross section SEM images of the LPG coated with [CHI/PAA]₂₀ multilayers.

Zeta-potential measurements were conducted during the deposition of CHI/PAA multilayers on Au NPs in order to monitor the LbL deposition process and evaluate the charge compensation mechanism for electrostatic assembly. Fig. 3. A depicts the procedure of sequential deposition of alternating CHI/PAA layers on the colloidal particles. Fig. 3. B shows changes in zeta-potential of Au NPs as they were coated with CHI/PAA multilayers. A negative zeta-potential of -25 mV was measured in 100 mM NaOAc buffer solution at pH 5 for the uncoated particles. The negative value of the surface charge is due to partially ionized carboxyl acid groups of citrate on the surface of Au NPs, which were originally introduced during the nanoparticle synthesis through the use of citrate as a reduction agent. The deposition of the first layer of chitosan switched the zeta potential to a positive value of +16 mV, indicating overcompensation of the surface charge by the cationic chitosan. Subsequent alternating depositions of polyelectrolyte layers via electrostatically driven sequential adsorption reversed the sign of zeta potential, consistent with a successful film buildup.

Fig. 3. (A) Schematic representation of LbL assembly of CHI/PAA films on Au NPs for zeta-potential measurements. (B) Zeta-potential measurements of bare Au NPs (1), and Au NPs coated with 1-4 layers of (2) Au NP/CHI, (3) Au NP/[CHI/PAA], (4) Au NP/[CHI/PAA/CHI] and (5) Au NP/[CHI/PAA]₂ at pH 5.

3.2. Salinity measurements with LbL-coated LPG fibers

The [CHI/PAA]₂₀-coated LPG fibers were used for the real-time, high-sensitivity salinity measurements in NaCl solutions. The response of coated LPG fibers in terms of RW shift recorded during the salinity measurement is shown in Fig. 4. The error bars are based on five measurements done on the same LPG. In order to compare and contrast the performance of the LPG with and without the stimuli-responsive thin film, the salinity sensing with bare LPG was also performed. The RI of NaCl solutions increases with salt concentration, resulting in a red shift of 2 nm/M in RW for bare LPG (Fig. 4, circles). With a [CHI/PAA]₂₀ film coating, the response of the fiber to varying NaCl concentrations was drastically enhanced compared to that of bare LPG. The coated LPG showed a salinity sensitivity of -36 nm shift/M, which was one order of magnitude higher than that of the bare LPG in the concentration range of 0.5-0.8 M. This salinity sensitivity is also one order of magnitude higher than the earlier reported salinity optical sensor with a sensitivity of 2 nm shift/M [15]. Interestingly, the salinity response of [CHI/ PAA]₂₀-coated LPG had two opposite trends, with a reversal point at 0.5 M (Fig. 4, squares): a red shift in the RW of LPG in the lower concentration range of 0.1 - 0.4M, and a blue shift in the higher concentration range from 0.5 to 0.8M. After each salinity measurement, the coated LPG was rinsed in a pH 7.5 phosphate buffer with no NaCl. The almost constant RW in the buffer solution (inset of Fig. 4) is a clear indication that the [CHI/PAA]₂₀ coating is stable throughout the salinity measurement. Importantly, the response of the LbL-coated fiber to ionic strength was fully reversible. It is important to note that while the LbL coating was always assembled at pH 5 (in the conditions when chitosan was water-soluble), the salinity measurements were first performed at pH 7.5 to closely mimic the seawater conditions.

Fig. 4. RW as a function of NaCl concentration for: [CHI/PAA]₂₀ coated LPG (squares) and bare LPG (circles). The inset to the upper left is the RW of coated LPG rinsed with pH 7.5 buffer after each

measurement and the insets to the lower left and upper right are the transmission spectra for the buffer solutions containing 0.1 - 0.4 M and 0.5-0.8 M NaCl in concentration, respectively.

More excitingly, the capability of LPG for real-time monitoring of LbL deposition and for a highly sensitive response of the coated fibers to salt concentrations affords us a powerful tool to probe the mechanism of the stimuli responsiveness and physiochemical properties of LbL films. Fig. 4 enables us to identify possible mechanisms associated with the ionic-strength responsiveness of the $[\text{CHI/PAA}]_n$ coating. The reversal point in the salinity response indicates that there are two distinct mechanisms or two “regions” in the ionic-strength responsiveness of $[\text{CHI/PAA}]_n$ thin film. We mark the red shift region at low NaCl concentrations of 0.1-0.4 M as Region I and the blue shift region at high NaCl concentrations of 0.5-0.8 M as Region II. In region I, the red shift is due to an increase in the effective refractive index of the coating, indicating a de-swelling of the thin film in response to the increase in NaCl concentration. This de-swelling behavior is usually associated with a decrease in the effective charge density on polyelectrolyte chains occurring as a result of screening of polyelectrolyte interactions with salt ions. As a result of such screening, a denser structure of the polyelectrolyte multilayers arises. In region II, the blue shift indicates a “loosening” or swelling of the multilayers in response to the further increase in NaCl concentration. The key to the emergence of a maximum in response of the multilayer-coated LPG fiber to ionic strength is in specific pH conditions used for film assembly and response. In particular, as shown in Fig. 4, the CHI/PAA films were assembled at pH 5, while ionic strength experiments were conducted at a high pH value of 7.5. Such post-assembly pH variations determine the charge state of weak polyelectrolyte multilayers [22] and are important for determining the LPG fiber salinity response. In order to better understand the mechanisms discussed above and in light of the importance of pH in determining the charge state of the polyelectrolytes [18], zeta-potential as a function of pH was measured for colloidal particles covered by a single layer of PAA and a single layer of CHI, respectively in Fig. 5.

Fig. 5. Zeta-potential of Au NPs covered by a layer of CHI (top) and a layer of PAA (bottom) as a function of pH.

Both CHI and PAA are weakly charged polyelectrolytes with respective pK_a values of 6.5 and 4.75 [23]. The $[\text{CHI/PAA}]_n$ multilayers were deposited at pH 5, where CHI and PAA are positively and negatively charged, respectively, as indicated by their respective zeta-potentials of +22 mV and -21 mV at pH 5 as shown in Fig. 5. During the film deposition at a constant pH, charge

compensation occurs through intrinsic mechanism, which includes matching the total number of ionized polymer units in the multilayers as polymer-polymer ionic pairs are formed [24]. As a result of charge neutrality within the LbL coating, the degree of swelling of these films is relatively low, with a typical water content in such films of 20-40% [25]. In the assembly conditions of pH 5, neither PAA nor CHI is completely ionized, however, and their unionized units which do not participate in ionic pairing are able to change their ionization and provide additional charge to the entire film when the solution pH is changed from that used in film assembly. After [CHI/PAA]_n film assembly, the solution pH is increased to 7.5 for salinity measurements. PAA is further ionized as indicated by the more negative zeta-potential of -33 mV, whereas CHI loses its positive charge as indicated by its less positive zeta potential of +3 mV. Such an increase in pH results in a multilayer with large number of excess negative charge supplied by ionized PAA units and thus a high degree of swelling due to the repulsion between the negatively charged, uncompensated PAA units, as depicted in Scheme 1, A. The PAA-containing multilayer is expected to swell at elevated pH due to the increased ionization of acrylic acid at such pH [22].

Scheme 1. Schematic representation of CHI/PAA multilayers exposed to solutions with no additional NaCl (A), low NaCl concentrations (B, Region I) and high NaCl concentrations (C, Region II) at pH 7.5.

Therefore, at pH 7.5 we have a polyelectrolyte network with considerable amount of uncompensated negative charge to begin with. In Region I, as NaCl ions are gradually added, the coating de-swells as negatively charged groups of COO⁻ in PAA chains are shielded by the sodium ions of salt solution in Scheme 1, B, known as the charge screening effect [26]. As a result of such charge screening by sodium ions, de-swelling of a single-component hydrogel LbL capsules composed of a similar polyanion of poly(methacrylic acid) (PMAA) have been previously reported [27]. An earlier study of hydrodynamic dimensions of PMAA chains also attributes salt-induced coil contraction to shielding of polyelectrolyte chain charges by salt ions [28]. In CHI/PAA films

at pH 7.5, de-swelling leads to a denser film with a higher effective refractive index and thus a red shift in the LPG RW.

In Region II, When the salt concentration increases up to 0.5 M, the long-range electrostatic repulsions between excess charges in the film are efficiently screened by the salt ions (an estimated Debye length does not exceed 4 Å). When the salt concentration increases to a degree relevant to that of seawater in the salinity measurement, salt ions start to affect interactions between CHI and PAA chains by breaking inter-polyelectrolyte ionic pairs [29, 30], as shown in Scheme 1, C. High salt concentrations are also known to decrease the tendency to form polymer complexes, dissociating polymer-polymer ionic pairing and diminishing the mutual attraction between polycations and polyanions [31]. In the [CHI/PAA]₂₀ coating, ionic doping increases the water content and causes film swelling as a result of a decreased number of polymer-polymer ionic pairs and increased osmotic pressure in the films. The film swelling leads to a decrease in the refractive index, thus a blue shift in the RW of coated LPG at high salt concentration. As we know, the most abundant dissolved ions in seawater are sodium (1.08 %), chloride (1.94 %), magnesium (0.12 %), sulfate (0.09 %), calcium (0.04 %), potassium (0.04 %) and bromide (0.0067 %) by mass percentage [32]. Since the concentration of sodium chloride in seawater is one order of magnitude higher than the second most abundant salt, the large shift of -36 nm/M obtained using NaCl solution is a clear indication of the excellent promise of the [CHI/PAA]₂₀-coated LPG for salinity measurements in seawater. Nevertheless, compared with monovalent sodium ion, divalent cations such as magnesium and calcium with higher ionic strengths can pair with carboxyl acid groups more strongly [33]. A higher degree of “loosening” or swelling in the CHI/PAA multilayers and consequently a higher LPG response could be anticipated if at a similar salt concentration. Despite

a lower concentration, a valuable next step is to incorporate salts of magnesium and calcium in the NaCl solution for further research and development of LbL-coated LPG salinity sensors.

The above discussion is based on the fact that the initial state of the polyelectrolyte coating is dominated by a large amount of free negative charge of PAA created by the pH change from 5 to 7.5. In order to provide an in-depth understanding of the swelling/de-swelling mechanism under different salt concentration, we next examine the effect of pH on the swelling/de-swelling behavior. However, it should be noted that current ocean pH is fairly stable, with only 0.1 variations in pH recorded at Ocean Station Aloha, for example [34]. This small pH variation induces a red shift of only 0.16 nm, insignificant compared to the high salinity response of -36 nm/M of our LbL-coated LPG. Cross sensitivity to pH of our LPG sensor can thus be ignored in the context of salinity measurements in seawater environment.

A change in pH of salinity measurements is expected to affect this excess charge and therefore change the salt-concentration dependence of the film swelling and fiber response. Two sets of experiments were designed to assess the pH effect. One is to measure the salinity response of [CHI/PAA]₂₀-coated LPG at pH 5, the pH value at which the LbL multilayers were assembled. Fig. 6. The error bars are based on five measurements done on the same LPG. A shows that contrary to what has been observed at pH 7.5, the RW of the coated fiber is significantly higher (1628.5 nm at pH 5 vs. 1568 nm at pH 7.5 for 0.1 M NaCl solutions), and there is a monotonic decrease in RW as salt concentration increases with no point of reversal. The lower RW of the coated fiber at pH 7.5 as compared to pH 5 is due to a decrease in the effective refractive index, a clear demonstration of a high degree of swelling at pH 7.5. As pH 5 is the assembly condition at which intrinsic charge compensation occurs, the assembled polyelectrolyte multilayer exhibits a low degree of swelling (and thus a high RW) due to extensive ionic pairing between oppositely charged polymer units. More importantly, salt response of the LbL-coated LPG fiber at pH 5 (Fig.

6) is drastically different from that observed at pH 7.5 (Fig. 4). Specifically, at increased salt concentrations, a monotonic decrease in the fiber RW, *i.e.* an enhanced uptake of water within LbL films, occurs at pH 5. Unlike the high density of unpaired ionic groups at pH 7.5, ionized groups are included within ionic pairs at pH 5, so that the addition of salt ions attacked polymer ion pairs immediately as it was added, resulting in the decrease of refractive index and a monotonic decrease as a function of salt concentration as depicted in Fig. 6. A.

Fig. 6. RW for the [CHI/ PAA]₂₀-coated fiber as a function of NaCl concentration measured in solutions at (A) pH 5 and (B) pH 3.5.

Finally, the salinity response of [CHI/PAA]₂₀-LPG at pH 3.5 was recorded. At this pH, the weak acid PAA is less ionized as indicated by the smaller number of negative zeta-potential of -10 mV in Fig. 5, whereas CHI is further ionized as indicated by its larger number of positive zeta-potential of +29 mV in Fig. 5, resulting in a multilayer with unpaired positive charges and thus a high degree of swelling due to the repulsion between ionized CHI molecules. The salinity response of the [CHI/PAA]₂₀ thus follows a similar trend with that measured at pH 7.5. That is, with the increase of the salt concentration, the film first shrinks due to charge screening by salt ions, and then swells at high salt concentrations due to ion doping which disrupts polymer-polymer ionic pairing. The only difference with the sensing at pH 7.5 is that the initial swelling is introduced by the excess positive charges of the CHI molecules at pH 3.5, rather than excess PAA charges at pH 7.5. Fig. 5. B shows the results of salinity measurements at pH 3.5. One can clearly see that there is a red shift in the RW at lower salt concentration and a blue shift at higher salt concentration, with 0.6 M as the reversal point, which is similar to that observed at pH 7.5. In addition to providing a robust salinity sensing platform, the LbL-coated LPG performed at different pH values afford a new angle in investigating the behavior of ionic-strength-responsive polyelectrolyte thin films as a function of multiple environmental parameters, such as ionic strength and pH. We should

note that the above discussion on the pH responsiveness of the coating is intended to provide an in-depth understanding of its swelling/de-swelling mechanism under different salt concentration. In fact, current ocean pH is fairly stable [34], and the cross sensitivity to pH of our LPG sensor can thus be ignored in the context of salinity measurements in seawater environment.

4. Conclusion

In this work, a highly sensitive salinity sensor based on [CHI/PAA]₂₀-coated LPG is demonstrated. It is the first report, to the best of our knowledge, on integration of the ionic-strength-responsive polyelectrolyte multilayers with LPG for salinity measurements. We have shown that the multilayer-enabled LPG exhibited a salinity sensitivity one order of magnitude higher than that achieved on the same LPG without coating as well as other reported fiber-optic salinity sensor. More interestingly, the response of the coated LPG in terms of RW shift occurred in two opposite directions at different ranges of salt concentration, with a red shift in the range of 0.1-0.4 M and a blue shift in the range of 0.5-0.8 M. The LbL-coated LPG readily affords an efficient tool to explore the effects of pH on the ionic-strength responsiveness of polyelectrolyte multilayers. Based on the measurements by coated LPG, we have shown that this two-region process depends on the pH values at which the LbL assembly and salinity measurements take place. When there is a difference in the pH values with extra charges introduced to the multilayers, the ionic-strength responsiveness undergoes a two-region process: shielding of excess charges resulting in the shrinking of the coating, and salt ion doping leading to an increase in the film water content. On the other hand, when the pH values are the same and there are minimum excess charges, the responsiveness is only through salt ion doping. The LbL/LPG is a powerful and real-time monitoring tool that allows better understanding of stimuli-responsive polyelectrolyte LbL assemblies useful for many applications such as the design and development of multifunctional

polyelectrolyte multilayer-based systems not only for robust salinity sensors but also for biomedicine and drug delivery.

Acknowledgements

Fan Yang is currently a PhD candidate of Materials Engineering at Stevens Institute of Technology. He received M.S. degree in Materials Science and Engineering in 2015 from Stevens Institute of Technology. His main areas of interests are the research and development of solar energy polymer materials, new polymer thin films of nanostructured functional coatings for optical fiber sensor applications.

Prof. Svetlana Sukhishvili earned her Ph.D. in Polymer Chemistry from the Moscow State University, Russia. After working as a Research Associate in the Department of Materials Science and Engineering, University of Illinois at Urbana-Champaign, she joined the Stevens Institute of Technology in 2000 as an Associate Professor, where she was promoted to Full Professor in 2008. She is now Full Professor in the Department of Materials Science and Engineering at Texas A&M University. Her research interests include responsive polymer-polymer and hybrid polymer-inorganic assemblies, controlled delivery materials, and nanotechnology-enabled sensing. She authored and co-authored several patents and over 100 research articles. She is a recipient of an Institutional Research Excellence Award, an Award for Distinguished Scientific Achievement from the American Coating Association, and holds an honorary degree from Stevens Institute Technology. She is a Fellow of the American Physical Society, and a recent recipient of a Special Creativity Award from the National Science Foundation.

Henry Du is a professor of Materials Engineering at Stevens Institute of Technology. He received his B.S. degree from South China University of Technology in 1982 and his Ph.D. degree from the Pennsylvania State University in 1988. His primary research areas include novel sensing platform, molecular and nanoscale surface functionalization, chemical and biological sensing and imaging.

Fei Tian is currently a research assistant professor of Materials Engineering at Stevens Institute of Technology. She received her B.S. degree in Electronic Information Science and Technology in 2005, M.S. degree in Microelectronics and Solid-State Electronics in 2009 from East China Normal University and Ph.D. degree in Materials Science and Engineering in 2013 from Stevens Institute of Technology. Her research interests include the investigation and development in the interface of photonics and functional nanomaterials and thin films at multi-length scales for applications in chemical and bio-sensing and drug release study.

This work is supported by the US National Science Foundation under grant number ECCS-1611155. We thank Kai Liu for providing the Au NPs in our experiment.

References

1. L. P. Knauth, Temperature and salinity history of the Precambrian ocean: implications for the course of microbial evolution, *Palaeogeogr. Palaeoclimatol. Palaeoecol.* 219, 53-69 (2005).
2. N. P. Fofonoff, Physical properties of seawater - a new salinity scale and equation of state for seawater, *J. Geophys. Res. Oceans* 90, 3332-3342 (1985).

3. N. H. Kenyon and R. H. Belderson, Bed forms of the Mediterranean undercurrent observed with side-scan sonar, *Sediment. Geol.* 9, 77-99 (1973).
4. A. Poisson, The Concentration of the KCl Solution Whose Conductivity Is That of Standard Seawater (35-Percent) at 15-Degrees-C, *IEEE J. Oceanic Eng.* 5, 24-28 (1980).
5. O. S. Wolfbeis, Fiber-optic chemical sensors and biosensors, *Anal. Chem.* 76, 3269-3283 (2004).
6. S. J. Zheng, Y. N. Zhu and S. Krishnaswamy, Fiber humidity sensors with high sensitivity and selectivity based on interior nanofilm-coated photonic crystal fiber long-period gratings, *Sens. Actuators, B* 176, 264-274 (2013).
7. S. J. Zheng, Long-period fiber grating moisture sensor with nano-structured coatings for structural health monitoring, *Struct Health Monit.* 14(2), 148-157 (2015).
8. J. L. Tang and J. N. Wang, Measurement of chloride-ion concentration with long-period grating technology, *Smart Mater. Struct.* 16, 665-672 (2007).
9. S. K. A. K. Bey, C. C. C. Lam, T. Sun and K. T. V. Grattan, Chloride ion optical sensing using a long period grating pair, *Sens. Actuators, A* 141, 390-395 (2008).
10. J. N. Wang, A microfluidic long-period fiber grating sensor platform for chloride ion concentration measurement, *Sensors (Basel)* 11, 8550-8568 (2011).
11. F. Tian, J. Kanka, B. Zou, K. S. Chiang and H. Du, Long-period gratings inscribed in photonic crystal fiber by symmetric CO₂ laser irradiation, *Opt. Express* 21, 13208-13218 (2013).
12. S. Zheng, B. Shan, M. Ghandehari and J. Ou, Sensitivity characterization of cladding modes in long-period gratings photonic crystal fiber for structural health monitoring, *Measurement* 72, 43-51 (2015).
13. F. Tian, J. Kanka, X. Z. Li and H. Du, Monitoring layer-by-layer assembly of polyelectrolyte multi-layers using high-order cladding mode in long-period fiber gratings, *Sens. Actuators, B* 196, 475-479 (2014).
14. G. R. C. Possetti, R. C. Kamikawachi, C. L. Prevedello, M. Muller and J. L. Fabris, Salinity measurement in water environment with a long period grating based interferometer, *Meas. Sci. Technol.* 20, 034003 (2009).
15. Q. Q. Meng, X. Y. Dong, K. Ni, Y. Li, B. Xu and Z. M. Chen, Optical fiber laser salinity sensor based on multimode interference effect, *IEEE Sens. J.* 14, 1813-1816 (2014).
16. M. C. Navarrete, N. Diaz-Herrera, A. Gonzalez-Cano and O. Esteban, A polarization-independent SPR fiber sensor, *Plasmonics* 5, 7-12 (2010).
17. F. Tian, J. Kanka, S. A. Sukhishvili and H. Du, Photonic crystal fiber for layer-by-layer assembly and measurements of polyelectrolyte thin films, *Opt. Lett.* 37, 4299-4301 (2012).
18. E. Guzman, J. A. Cavallo, R. Chulia-Jordan, C. Gomez, M. C. Strumia, F. Ortega and R. G. Rubio, pH-induced changes in the fabrication of multilayers of poly(acrylic acid) and chitosan: fabrication, properties, and tests as a drug storage and delivery system, *Langmuir* 27, 6836-6845 (2011).
19. R. Chester. *Marine geochemistry* (John Wiley & Sons, 2009).
20. R. A. Rosson, B. M. Tebo and K. H. Nealson, Use of poisons in determination of microbial manganese binding rates in seawater, *Appl. Environ. Microbiol.* 47, 740-745 (1984).
21. P. Pinkhasova, L. Yang, Y. Zhang, S. Sukhishvili and H. Du, Differential SERS activity of gold and silver nanostructures enabled by adsorbed poly (vinylpyrrolidone), *Langmuir* 28, 2529-2535 (2012).
22. C. Déjugnat and G. B. Sukhorukov, pH-responsive properties of hollow polyelectrolyte microcapsules templated on various cores, *Langmuir* 20, 7265-7269 (2004).
23. H. R. Lin, S. P. Yu, C. J. Kuo, H. J. Kao, Y. L. Lo, and Y. J. Lin, Pilocarpine-loaded chitosan-PAA nanosuspension for ophthalmic delivery, *J. Biomater. Sci., Polym. Ed.* 18, 205-221 (2007).
24. J. B. Schlenoff, Charge Balance and Transport in Polyelectrolyte Multilayers, in *Multilayer Thin Films* (Wiley-VCH Verlag GmbH & Co. KGaA, 2003), pp. 99-132.
25. O. M. Tanchak, and C. J. Barrett, "Swelling dynamics of multilayer films of weak polyelectrolytes," *Chem. Mater.* 16, 2734-2739 (2004).
26. Y. Chen, and H. M. Tan, Crosslinked carboxymethylchitosan-g-poly(acrylic acid) copolymer as a novel superabsorbent polymer, *Carbohydr. Res.* 341, 887-896 (2006).
27. V. Kozlovskaya, E. Kharlampieva, M. L. Mansfield, and S. A. Sukhishvili, "Poly(methacrylic acid) hydrogel films and capsules: Response to pH and ionic strength, and encapsulation of macromolecules," *Chem. Mater.* 18, 328-336 (2006).

28. D. Pristinski, V. Kozlovskaya, and S. A. Sukhishvili, "Fluorescence correlation spectroscopy studies of diffusion of a weak polyelectrolyte in aqueous solutions," *J. Chem. Phys.* 122, 14907 (2005).
29. Q. F. Wang and J. B. Schlenoff, The Polyelectrolyte Complex/Coacervate Continuum, *Macromolecules* 47, 3108-3116 (2014).
30. P. K. Jha, P. S. Desai, J. Y. Li and R. G. Larson, pH and Salt Effects on the Associative Phase Separation of 28
31. J. T. Overbeek and M. J. Voorn, Phase separation in polyelectrolyte solutions: theory of complex coacervation, *J. Cell. Physiol.* 49, 7-22; discussion, 22-26 (1957).
32. A. G. Dickson and C. Goyet, Handbook of Methods for the Analysis of the Various Parameters of the Carbon Dioxide System in Sea Water, U.S. Department of Energy, Oak Ridge, TN (1994).
33. M. Zhang, Z. Cheng, T. Zhao, M. Liu, M. Hu and J. Li, Synthesis, characterization, and swelling behaviors of salt-sensitive maize bran–poly (acrylic acid) superabsorbent hydrogel, *J. Agric. Food. Chem.* 62, 8867-8874 (2014).
34. D. H. Levinson and J. H. Lawrimore, State of the climate in 2007, *Bull. Am. Meteorol. Soc.* 89, S1-S179 (2008).

Figure Caption

Fig. 1. LPG transmission spectra for the monitoring of the LbL assembly of CHI/PAA multilayers on SMF-28 with LPG at pH 5.

Fig. 2. The cross section SEM images of the LPG coated with [CHI/PAA]₂₀ multilayers.

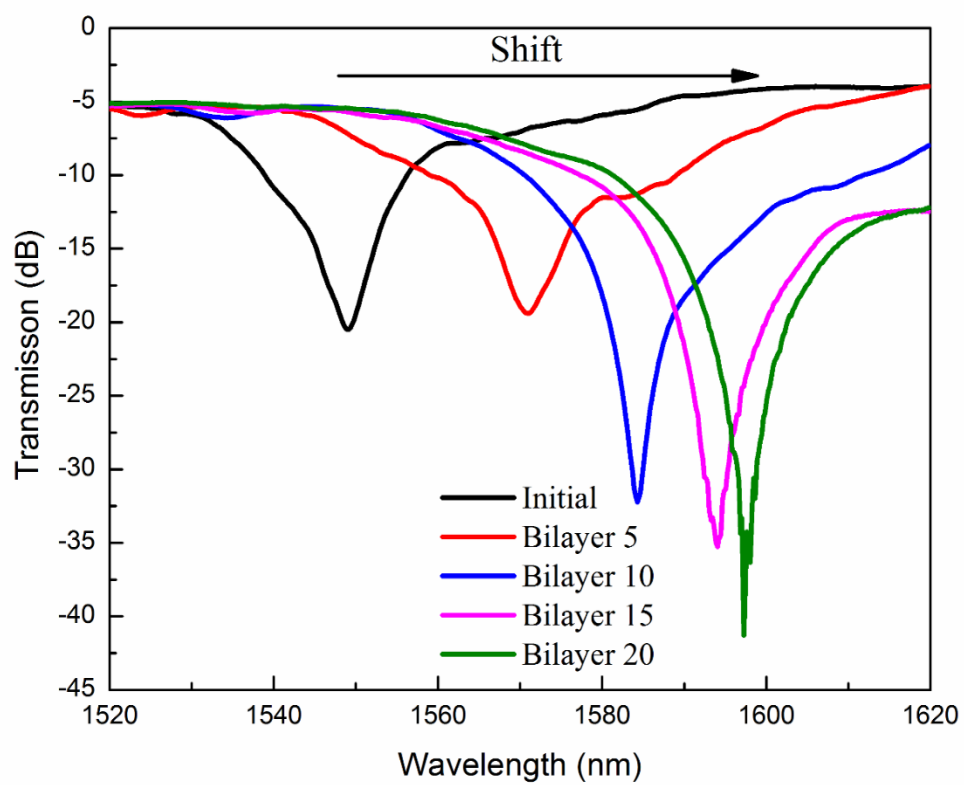
Fig. 3. (A) Schematic representation of LbL assembly of CHI/PAA films on Au NPs for zeta-potential measurements. (B) Zeta-potential measurements of bare Au NPs (1), and Au NPs coated with 1- 4 layers of (2) Au NP/CHI, (3) Au NP/[CHI/PAA], (4) Au NP/[CHI/PAA/CHI] and (5) Au NP/[CHI/PAA]₂ at pH 5.

Fig. 4. RW as a function of NaCl concentration for: [CHI/PAA]₂₀ coated LPG (squares) and bare LPG (circles). The inset to the upper left is the RW of coated LPG rinsed with pH 7.5 buffer after each measurement and the insets to the lower left and upper right are the transmission spectra for the buffer solutions containing 0.1 - 0.4 M and 0.5-0.8 M NaCl in concentration, respectively.

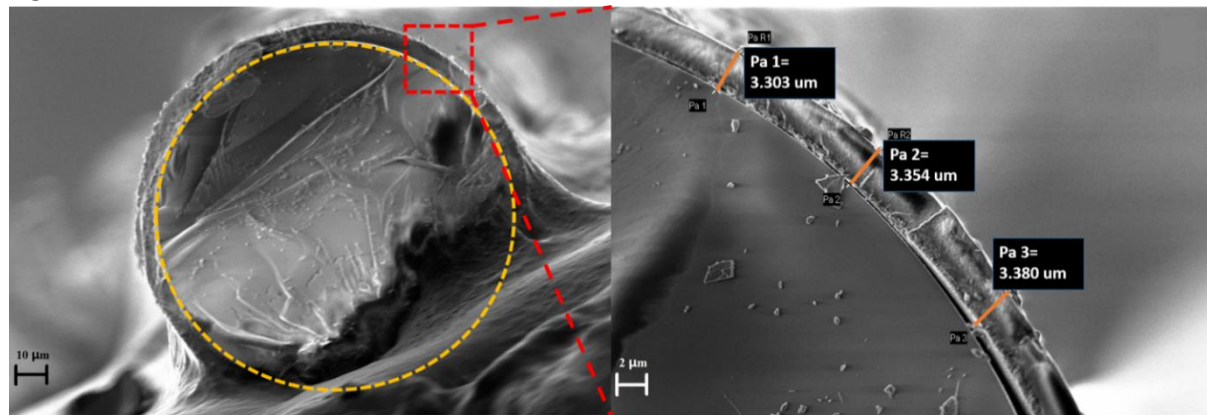
Fig. 5. Zeta-potential of Au NPs covered by a layer of CHI (top) and a layer of PAA (bottom) as a function of pH.

Scheme 1. Schematic representation of CHI/PAA multilayers exposed to solutions with no additional NaCl (A), low NaCl concentrations (B, Region I) and high NaCl concentrations (C, Region II) at pH 7.5.

Fig-1



Figr-2



Figr-3

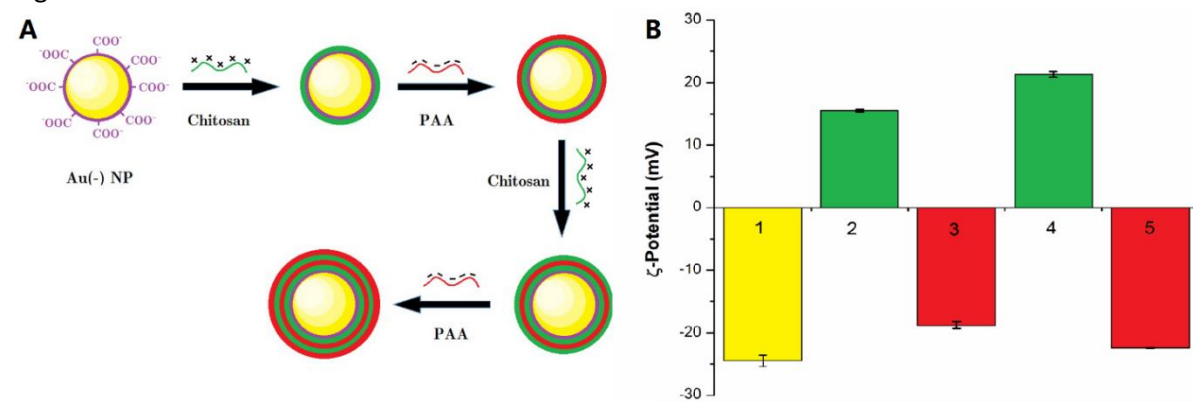
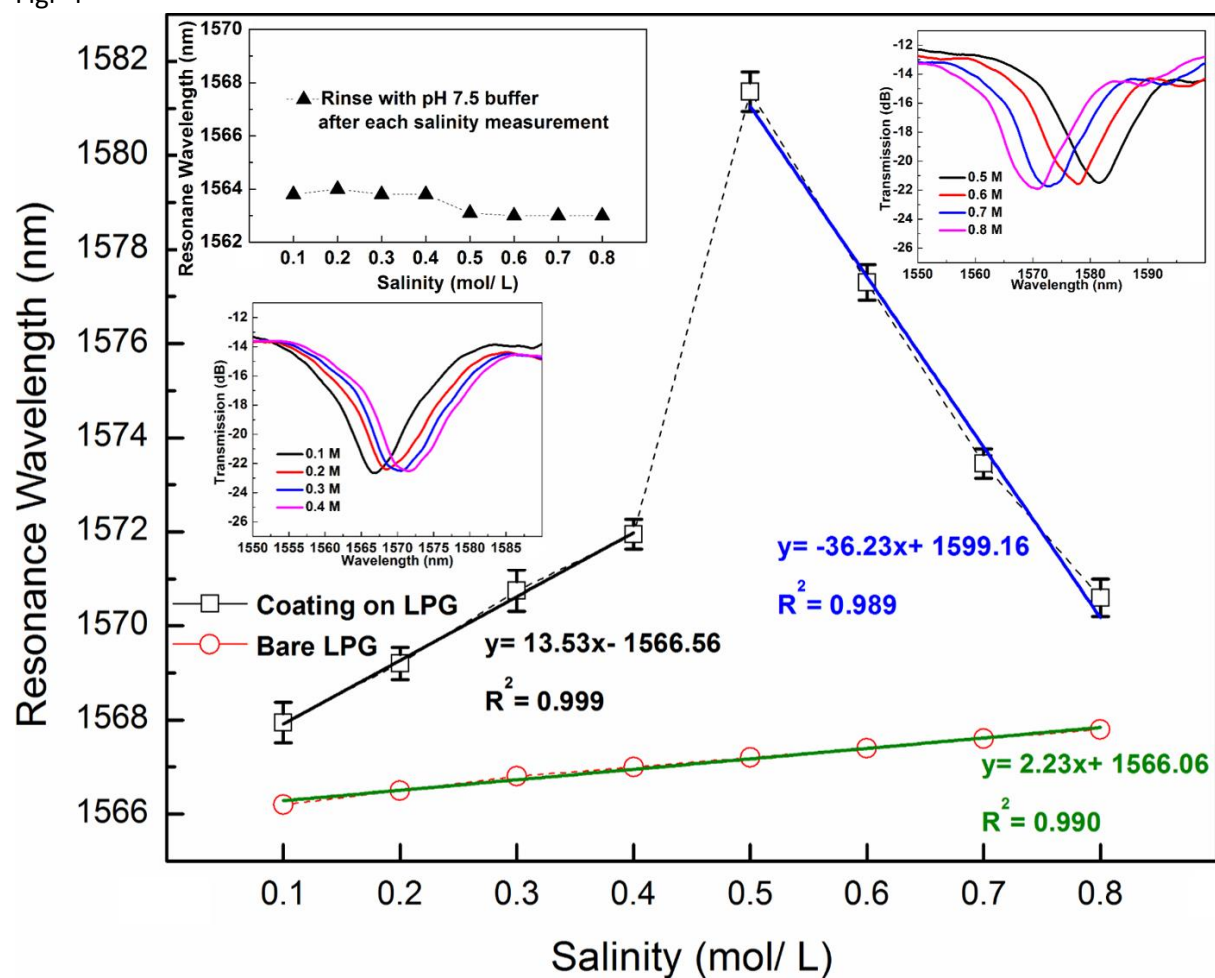
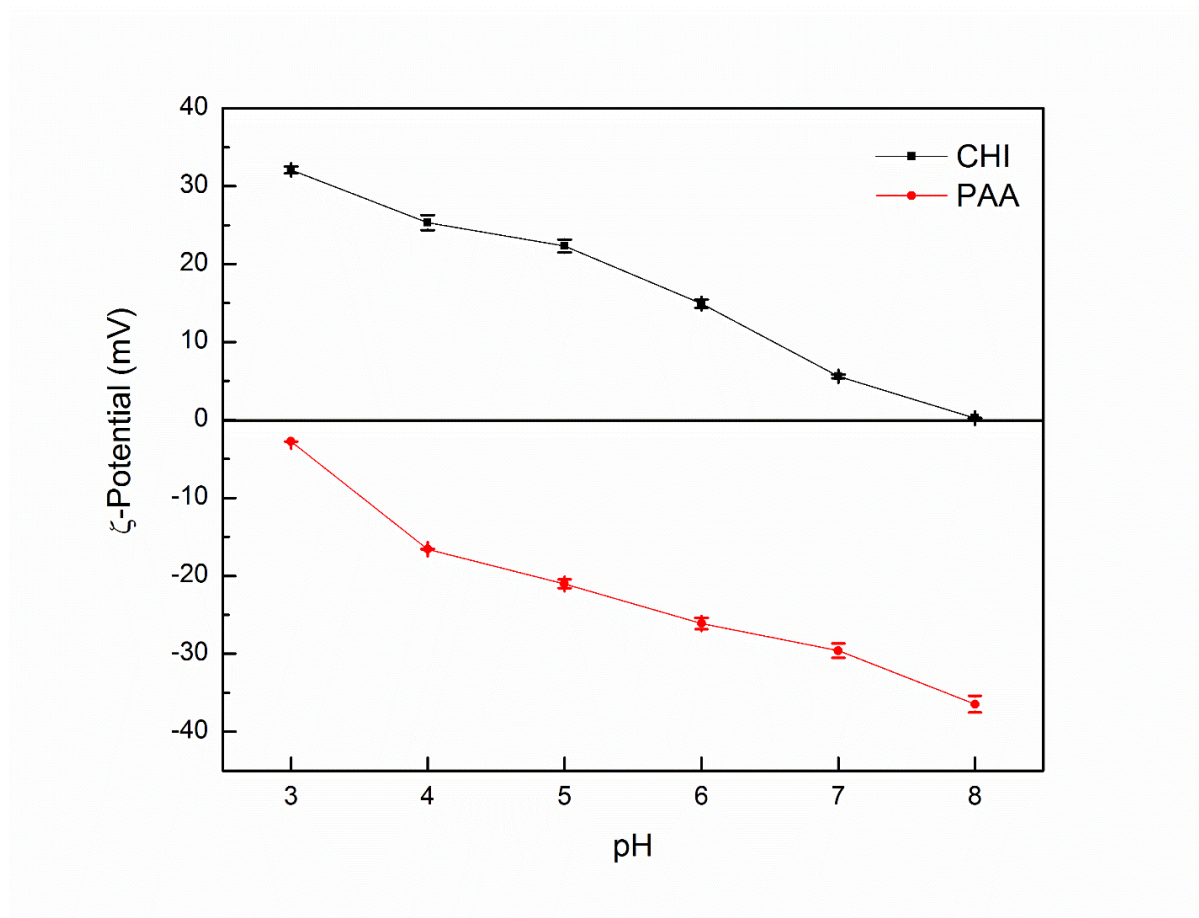


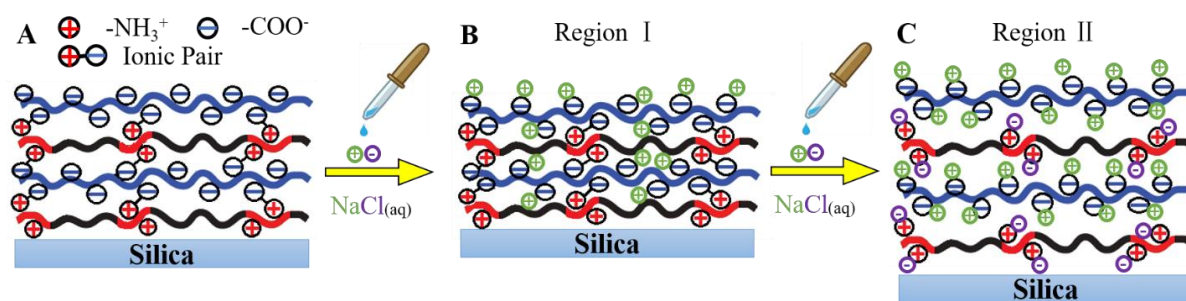
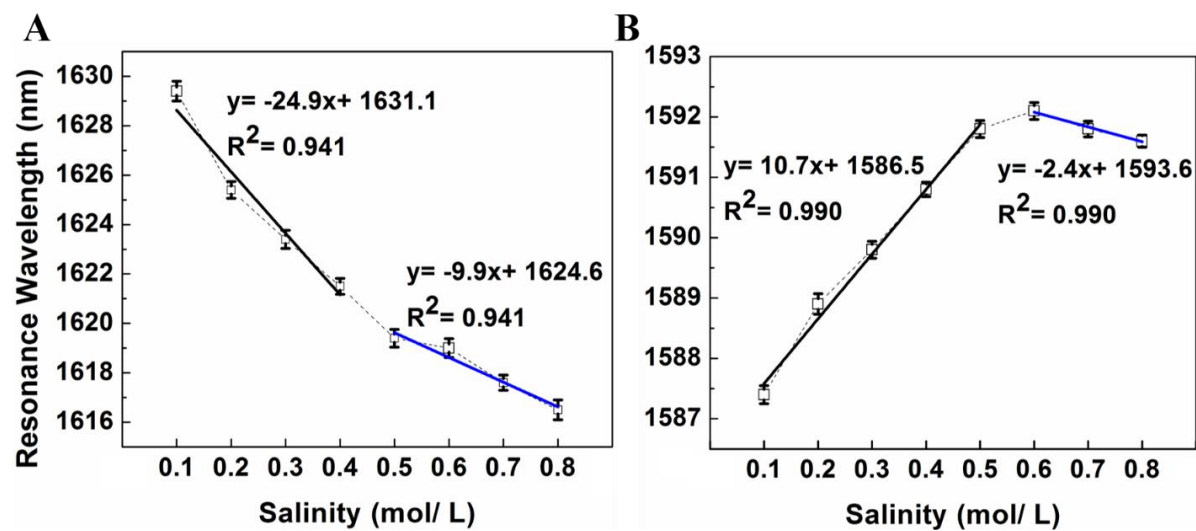
Fig-4



Figr-5



Figr-6



Scheme 1a

